

Zee-Babu model in a non-holomorphic modular A_4 symmetry and modular stabilization

Tatsuo Kobayashi,^{1,*} Hiroshi Okada,^{2,†} and Yuta Orikasa^{3,‡}

¹*Department of Physics, Hokkaido University, Sapporo 060-0810, Japan*

²*Department of Physics, Henan Normal University, Xinxiang 453007, China*

³*Institute of Experimental and Applied Physics,*

Czech Technical University in Prague,

Husova 240/5, 110 00 Prague 1, Czech Republic

(Dated: February 19, 2025)

Abstract

We study a Zee-Babu neutrino model in a non-holomorphic modular A_4 symmetry, and we construct a model so that there are minimum free parameters (two complex parameters). We find only the normal hierarchy is allowed. Moreover, the allowed region to satisfy the neutrino oscillation data is localized at nearby $\tau = \omega$. The small absolute deviation plays a crucial role in fitting two mixings of s_{23}^2 and s_{12}^2 . In addition, we obtain several predictions on Majorana and Dirac CP phases, and neutrinoless double beta decay as shown in our chi square numerical analysis. We also study modulus stabilization within the framework of non-supersymmetric models. In the end, we compute the expansion of modular forms at nearby $\tau = \omega$ in the Appendix so that one can apply them for a model and understand its analytical structure.

*Electronic address: kobayashi@particle.sci.hokudai.ac.jp

†Electronic address: hiroshi3okada@htu.edu.cn

‡Electronic address: Yuta.Orikasa@utef.cvut.cz

I. INTRODUCTION

A radiative seesaw model is one of the promising candidates to understand the tiny active neutrino masses in a low energy theory that reaches at current experiments such as CERN large hadron collider. In particular, Zee-Babu(ZB) neutrino model provides the neutrino mass matrix at two-loop level as a leading contribution only by introducing a singly-charged boson S^- and a doubly-charged boson k^{++} , and it does not require any additional symmetries to forbid tree level or one-loop level neutrino masses [1, 2]. Moreover, the ZB model has two remarkable features. The first one is that the lightest neutrino mass eigenvalue is zero because of the rank-two neutrino mass matrix that arises from anti-symmetric Yukawa $f \overline{L}_{Li} f_{ij} L_{Lj}^c S^+$. It implies that the two non-vanishing neutrino mass eigenvalues are uniquely determined by inputting two observables, that is, solar and atmospheric mass square differences. The second one is that the neutrino mass matrix is close to type- A_1 texture [3] if all the free parameters are order one under the assumption of diagonal charged-lepton mass matrix. Type- A_1 texture is given by

$$\begin{pmatrix} 0 & 0 & \times \\ 0 & \times & \times \\ 0 & \times & \times \end{pmatrix}, \quad (\text{I.1})$$

where \times is a non-zero component. This texture does not allow the inverted hierarchy via current experiments.¹ This texture in ZB model comes from the fact that the neutrino mass matrix is proportional to the following mass matrix;

$$\frac{1}{M} \begin{pmatrix} m_e^2 & m_e m_\mu & m_e m_\tau \\ m_e m_\mu & m_\mu^2 & m_\mu m_\tau \\ m_e m_\tau & m_\mu m_\tau & m_\tau^2 \end{pmatrix}, \quad (\text{I.2})$$

where M is the mass of singly or doubly charged bosons, and m_e, m_μ, m_τ is measured charged-lepton masses. Even though the ZB model already has some advantages on the lepton masses and mixings mentioned above, there still exists space to reduce free parameters to get more predictions.

In this paper, we apply a non-holomorphic modular A_4 flavor symmetry for the ZB model and investigate its nature of the lepton sector. For the last several years, modular

¹ In details, see e.g. ref [3].

flavor symmetric models have been being studied intensively [4]. In those models, Yukawa couplings and masses are functions of the modulus τ and written by holomorphic modular forms of S_3 , A_4 , S_4 , A_5 and others [4–7]. Phenomenologically interesting results have been obtained within the framework of supersymmetric models. (See for reviews refs. [8, 9].) The non-holomorphic modular symmetry was recently formulated by Qu and Ding [10], which can be applicable to non-supersymmetric theories without any potential difficulties. That has extended the possibilities for model building including non-supersymmetric models with Yukawa couplings and masses of positive and negative weights. Richer flavor structures can be realized by use of non-holomorphic modular forms.² After ref. [10], several ideas have been arisen in refs. [12–17]. The non-holomorphic groups provide negative modular forms which do not have in holomorphic one.³ Thus, one expects different kinds of predictions would be obtained. In fact, we discover that our scenario has sharp predictions on mixing angles and phases only at nearby $\tau = \omega$, where $\omega = e^{2\pi i/3}$. Here, we perform chi square numerical analysis and compare with predictions at $\tau = \omega$. Then, we find the small deviation crucially contributes to two reliable observables s_{23}^2 and s_{12}^2 . We also discuss the modulus stabilization at nearby $\tau = \omega$ within the framework of non-supersymmetric models.

This paper is organized as follows. In Sec. II, we give a brief review on the modular symmetry and modular forms. In Sec. III, we explain our model, constructing the valid charged-lepton Yukawa sector, Higgs potential, and active neutrino sector. In the neutrino sector, we show several relations coming from features of the Zee-Babu model and modular A_4 symmetry. Then, we perform the $\Delta\chi^2$ analysis to get our results, comparing the result of $\tau = \omega$. In Sec. IV, we study the modulus stabilization at nearby $\tau = \omega$ in non-supersymmetric models. We have conclusions and discussion in Sec. V. Appendix A shows A_4 modular forms, which we use. In Appendix B, we show helpful formalisms which are expanded at nearby $\tau = \omega$.

² When we start with supersymmetric models, supersymmetry breaking effects may affect the flavor structure at low-energy scale [11].

³ Note that the non-holomorphic modular symmetries include nature of holomorphic one.

II. MODULAR SYMMETRY AND MODULAR FORMS

We start with the homogeneous modular group $\Gamma = SL(2, \mathbb{Z})$, which is the special linear group of 2×2 matrices with integer entries,

$$\gamma = \begin{pmatrix} a & b \\ c & d \end{pmatrix}, \quad (\text{II.1})$$

where $ad - bc = 1$. This group is generated by the following two generators:

$$S = \begin{pmatrix} 0 & 1 \\ -1 & 0 \end{pmatrix}, \quad T = \begin{pmatrix} 1 & 1 \\ 0 & 1 \end{pmatrix}. \quad (\text{II.2})$$

They satisfy the following algebraic relations:

$$S^2 = -\mathbf{1}, \quad (ST)^3 = \mathbf{1}, \quad (\text{II.3})$$

where $\mathbf{1}$ is the identity. The modular group includes the principal congruence subgroup of the level N , $\Gamma(N)$, which is defined by

$$\Gamma(N) = \left\{ \begin{pmatrix} a & b \\ c & d \end{pmatrix} \in \Gamma, \quad \begin{pmatrix} a & b \\ c & d \end{pmatrix} = \begin{pmatrix} 1 & 0 \\ 0 & 1 \end{pmatrix} \pmod{N} \right\}. \quad (\text{II.4})$$

The quotients $\Gamma_N = \Gamma / \pm \Gamma(N)$ are isomorphic to S_3 , A_4 , S_4 , and A_5 [18].⁴ In our model, we use $\Gamma_3 \simeq A_4$.

The modulus τ transforms

$$\tau \rightarrow \gamma\tau = \frac{a\tau + b}{c\tau + d}, \quad (\text{II.5})$$

under the modular symmetry. Note that the point $\tau = \omega$ is the fixed point of the (ST) transformation, where \mathbb{Z}_3 symmetry remains. Also, the point $\tau = i$ is the fixed point of S . Moreover, the T symmetry remains in the limit $\text{Im}\tau \rightarrow \infty$.

The modular forms of weight k at level N transforms

$$Y_{\mathbf{r}}^{(k)}(\tau) \rightarrow Y_{\mathbf{r}}^{(k)}(\gamma\tau) = (c\tau + d)^k \rho_{\mathbf{r}}(\gamma) Y_{\mathbf{r}}^{(k)}(\tau), \quad (\text{II.6})$$

⁴ These non-Abelian groups have been used to explain the flavor structures of quarks and leptons [19–25].

	\overline{L}_L	ℓ_R	H	S^-	k^{++}
$SU(2)_L$	2	1	2	1	1
$U(1)_Y$	$\frac{1}{2}$	-1	$\frac{1}{2}$	-1	+2
A_4	3	3	1	1	1
$-k_I$	-1	+1	0	+2	0

TABLE I: Charge assignments of the SM leptons \overline{L}_L and ℓ_R and Δ under $SU(2)_L \otimes U(1)_Y \otimes A_4$ where $-k_I$ is the number of modular weight. Note here that all the bosons are assigned to be trivial singlet **1**.

where $\rho_{\mathbf{r}}(\gamma)$ is a unitary matrix corresponding to the representation \mathbf{r} of Γ_N . For $k > 0$, modular forms are holomorphic. One can define non-holomorphic modular forms for $k \leq 0$, i.e. polyharmonic Maaß forms. They satisfy the following Laplacian condition [10]:

$$\left(-4y^2 \frac{\partial}{\partial \tau} \frac{\partial}{\partial \bar{\tau}} + 2iky \frac{\partial}{\partial \bar{\tau}}\right) Y_{\mathbf{r}}^{(k)}(\tau) = 0, \quad (\text{II.7})$$

where $\tau = x + iy$, and the proper growth condition,

$$Y_{\mathbf{r}}^{(k)}(\tau) = \mathcal{O}(y^\alpha), \quad (\text{II.8})$$

as $y \rightarrow \infty$ for some α . The polyharmonic Maaß forms are non-holomorphic.

Matter fields ϕ of the weight k and the representation \mathbf{r} also transform as

$$\phi \rightarrow (c\tau + d)^k \rho_{\mathbf{r}}(\gamma) \phi, \quad (\text{II.9})$$

under the modular symmetry.

We study a model with the $\Gamma_3 \simeq A_4$ symmetry. Some modular forms of the level $N = 3$ are shown in Appendix A.

III. MODEL SETUP

Here, we explain our setup based on the ZB model with a non-holomorphic modular A_4 symmetry. Left-handed leptons, which are denoted by $\overline{L}_L \equiv [\bar{\nu}_L, \bar{\ell}_L]^T$, are assigned to A_4 triplet with -1 modular weight. The right-handed charged-leptons, ℓ_R , are assigned to A_4 triplet with $+1$ modular weight. The singly-charged S^- and doubly-charged bosons k^{++}

respectively have +2 and 0 modular weights. Note here that all the bosons are assigned to be trivial singlet $\mathbf{1}$. The standard model Higgs is denoted by $H \equiv [w^+, (v, h + iz)/\sqrt{2}]^T$ where w^+ and z respectively give the gauge masses of W^+ and Z in the standard model after the spontaneous symmetry breaking. The field contents and their assignments are summarized in Tab. I.

A. Charged-lepton mass matrix

Under these symmetries, we write the renormalizability relevant Lagrangian for charged-leptons is found as follows:

$$\begin{aligned}
& a_e(\overline{L}_{L_e}e_R + \overline{L}_{L_\mu}\tau_R + \overline{L}_{L_\tau}\mu_R)H + b_e [y_1(2\overline{L}_{L_e}e_R - \overline{L}_{L_\mu}\tau_R - \overline{L}_{L_\tau}\mu_R) \\
& + y_2(2\overline{L}_{L_\mu}\mu_R - \overline{L}_{L_e}\tau_R - \overline{L}_{L_\tau}e_R) + y_3(2\overline{L}_{L_\tau}\tau_R - \overline{L}_{L_e}\mu_R - \overline{L}_{L_\mu}e_R)] H \\
& + c_e [y_1(\overline{L}_{L_\tau}\mu_R - \overline{L}_{L_\mu}\tau_R) + y_2(\overline{L}_{L_\tau}e_R - \overline{L}_{L_e}\tau_R) + y_3(\overline{L}_{L_e}\mu_R - \overline{L}_{L_\mu}e_R)] H + \text{h.c.}, \quad (\text{III.1})
\end{aligned}$$

where $Y_3^{(0)} \equiv [y_1, y_2, y_3]^T$ [10]. (See Appendix A.) After the spontaneous symmetry breaking of H , the charged-lepton mass matrix M_ℓ is given by

$$M_\ell = \frac{v}{\sqrt{2}} \left[a_e \begin{pmatrix} 1 & 0 & 0 \\ 0 & 0 & 1 \\ 0 & 1 & 0 \end{pmatrix} + b_e \begin{pmatrix} 2y_1 & -y_3 & -y_2 \\ -y_3 & 2y_2 & -y_1 \\ -y_2 & -y_1 & 2y_3 \end{pmatrix} + c_e \begin{pmatrix} 0 & y_3 & -y_2 \\ -y_3 & 0 & y_1 \\ y_2 & -y_1 & 0 \end{pmatrix} \right], \quad (\text{III.2})$$

where a_e, b_e, c_e , which are real parameters without loss of generality, are determined in order to fix the mass eigenvalues of charged-leptons. Inputting the experimental masses of charged-leptons and a value of τ , these free parameters are numerically solved by the following three relations:

$$\text{Tr}[M_\ell M_\ell^\dagger] = |m_e|^2 + |m_\mu|^2 + |m_\tau|^2, \quad (\text{III.3})$$

$$\text{Det}[M_\ell M_\ell^\dagger] = |m_e|^2 |m_\mu|^2 |m_\tau|^2, \quad (\text{III.4})$$

$$(\text{Tr}[M_\ell M_\ell^\dagger])^2 - \text{Tr}[M_\ell M_\ell^\dagger]^2 = 2(|m_e|^2 |m_\mu|^2 + |m_\mu|^2 |m_\tau|^2 + |m_e|^2 |m_\tau|^2). \quad (\text{III.5})$$

Here, M_e is diagonalized by bi-unitary mixing matrices as $D_\ell \equiv \text{diag}(m_e, m_\mu, m_\tau) = V_{eL}^\dagger M_\ell V_{eR}$.

B. Higgs potential

Renormalizable Higgs potential is given by

$$\mathcal{V} = -\mu_H^2 |H|^2 - \mu_S^2 |S^-|^2 - \mu_k^2 |k^{++}|^2 + (\mu s^- s^- k^{++} + \text{h.c.}) \quad (\text{III.6})$$

$$+ \lambda_H |H|^4 + \lambda_S |S^-|^4 + \lambda_k |k^{++}|^4 + \lambda_{HS} |H|^2 |S^-|^2 + \lambda_{Hk} |H|^2 |k^{++}|^2 + \lambda_{Sk} |S^-|^2 |k^{++}|^2, \quad (\text{III.7})$$

where $\mu_S^2 \equiv \mu_{S_0}^2 (\tau - \bar{\tau})^2$, $\mu \equiv \mu_0 Y_1^{(-4)}$, $\lambda_S \equiv \lambda_{S_0} |(\tau - \bar{\tau})^2|^2$, $\lambda_{HS} \equiv \lambda_{HS_0} (\tau - \bar{\tau})^2$, $\lambda_{Sk} \equiv \lambda_{Sk_0} (\tau - \bar{\tau})^2$ in order to be invariant under the modular symmetry. After spontaneous symmetry breaking by H , physical Higgs masses are found as

$$m_H^2 = \lambda_H v^2, \quad (\text{III.8})$$

$$m_s^2 = -\mu_S^2 + \frac{\lambda_{HS}}{2} v^2, \quad (\text{III.9})$$

$$m_k^2 = -\mu_k^2 + \frac{\lambda_{Hk}}{2} v^2. \quad (\text{III.10})$$

C. Active neutrino mass matrix

The valid Lagrangian for the neutrino sector is found as follows:

$$\begin{aligned} -\mathcal{L}_\nu &= a_s \left[y_1 (\overline{L_{L\mu}} \cdot L_{L\tau}^c - \overline{L_{L\tau}} \cdot L_{L\mu}^c) \right. \\ &\quad \left. + y_2 (\overline{L_{L\tau}} \cdot L_{Le}^c - \overline{L_{Le}} \cdot L_{L\tau}^c) + y_3 (\overline{L_{Le}} \cdot L_{L\mu}^c - \overline{L_{L\mu}} \cdot L_{Le}^c) \right] S^- \\ &\quad + a_k \left[y'_1 (2\overline{e_R^c} e_R - \overline{\mu_R^c} \tau_R - \overline{\tau_R^c} \mu_R) \right. \\ &\quad \left. + y'_2 (2\overline{\mu_R^c} \mu_R - \overline{e_R^c} \tau_R - \overline{\tau_R^c} e_R) + y'_3 (2\overline{\tau_R^c} \tau_R - \overline{e_R^c} \mu_R - \overline{\mu_R^c} e_R) \right] k^{++} \end{aligned} \quad (\text{III.11})$$

$$+ b_k \left[\overline{e_R^c} e_R + \overline{\mu_R^c} \tau_R + \overline{\tau_R^c} \mu_R \right] k^{++} + \text{h.c.} \quad (\text{III.12})$$

$$= a_s \left[\overline{\nu_L} f V_{eL}^* \ell_L^c + \overline{\ell_L} V_{eL}^\dagger f^T \nu_L^c \right] S^- + a_k \overline{\ell_R^c} V_{eR}^T V_{eR} \ell_R k^{++} + \text{h.c.}, \quad (\text{III.13})$$

where we define $\ell_{L/R} \equiv [e, \mu, \tau]_{L,R}^T$ which are mass eigenstates of the charged-leptons in the last line, $\cdot \equiv i\tau_2$, where τ_2 is second Pauli matrix, and $Y_3^{(-2)} \equiv [y'_1, y'_2, y'_3]^T$ [10]. (See

Appendix A.) Then, the neutrino mass matrix is given at two-loop level as follows:

$$(m_\nu)_{ij} \simeq \frac{\mu^*}{64\pi^2} \frac{a_s^2 a_k}{m_s^2} I(r) \left[f V_{eL}^* D_\ell^* V_{eR}^T V_{eR} D_\ell^\dagger V_{eL}^\dagger f^T \right]_{ij} \equiv \kappa \left[f M_\ell^* g M_\ell^\dagger f^T \right]_{ij}, \quad (\text{III.14})$$

$$I(r) = - \int_0^1 dx \int_0^{1-x} dy \frac{1-y}{x+(r-1)y+y^2} \ln \left[\frac{y(1-y)}{x+ry} \right], \quad (\text{III.15})$$

$$f = \begin{pmatrix} 0 & y_3 & -y_2 \\ -y_3 & 0 & y_1 \\ y_2 & -y_1 & 0 \end{pmatrix}, \quad g = \begin{pmatrix} 2y'_1 & -y'_3 & -y'_2 \\ -y'_3 & 2y'_2 & -y'_1 \\ -y'_2 & -y'_1 & 2y'_3 \end{pmatrix} + \tilde{b}_k \begin{pmatrix} 1 & 0 & 0 \\ 0 & 0 & 1 \\ 0 & 1 & 0 \end{pmatrix}, \quad (\text{III.16})$$

where $\tilde{b}_k \equiv b_k/a_k$, $r \equiv m_k^2/m_s^2$. Since the loop function $I(r)$ does not depend on the masses of charged-leptons in the limit of $\frac{m_{e,\mu,\tau}}{m_{s,k}} \ll 1$, one can redefine $m_\nu \equiv \kappa \tilde{m}_\nu$. Since the coupling f is an anti-symmetric matrix that is rank two, \tilde{m}_ν has one vanishing mass eigenvalue. Therefore, we find

$$(\text{NH}) : \quad U_\nu^T \tilde{m}_\nu U_\nu = \text{diag}(0, \tilde{D}_{\nu_2}, \tilde{D}_{\nu_3}), \quad (\text{III.17})$$

$$(\text{IH}) : \quad U_\nu^T \tilde{m}_\nu U_\nu = \text{diag}(\tilde{D}_{\nu_1}, \tilde{D}_{\nu_2}, 0). \quad (\text{III.18})$$

In this case, one can write κ^2 in terms of either of two mass squared differences Δm_{atm}^2 and Δm_{sol}^2 , and mass eigenvalues of \tilde{m}_ν as follows:

$$(\text{NH}) : \quad \kappa^2 = \frac{|\Delta m_{\text{atm}}^2|}{\tilde{D}_{\nu_3}^2}, \quad (\text{IH}) : \quad \kappa^2 = \frac{|\Delta m_{\text{atm}}^2|}{\tilde{D}_{\nu_2}^2}, \quad (\text{III.19})$$

where we choose Δm_{atm}^2 as an input observable. Applying Eq. (III.19), Δm_{sol}^2 is given by

$$(\text{NH}) : \quad \Delta m_{\text{sol}}^2 = \kappa^2 \tilde{D}_{\nu_2}^2 = \frac{\tilde{D}_{\nu_2}^2}{\tilde{D}_{\nu_3}^2} |\Delta m_{\text{atm}}^2|, \quad (\text{III.20})$$

$$(\text{IH}) : \quad \Delta m_{\text{sol}}^2 = \kappa^2 (\tilde{D}_{\nu_2}^2 - \tilde{D}_{\nu_1}^2) = \left(1 - \frac{\tilde{D}_{\nu_1}^2}{\tilde{D}_{\nu_2}^2} \right) |\Delta m_{\text{atm}}^2|. \quad (\text{III.21})$$

Sum of neutrino masses $\sum D_{\nu_i}$ is found as follows:

$$(\text{NH}) : \quad \sum D_{\nu_i} \sim \sqrt{\Delta m_{\text{atm}}^2}, \quad (\text{III.22})$$

$$(\text{IH}) : \quad \sum D_{\nu_i} \sim 2\sqrt{\Delta m_{\text{atm}}^2}. \quad (\text{III.23})$$

This observable would favor a recent result of DESI and CMB data combination that provides the upper bound $\sum D_\nu \leq 72$ meV [26].

The observed mixing matrix is defined by $U = V_{eL}^\dagger V_\nu$ [27] and the mixings are given in terms of the component of U as follows:

$$\sin^2 \theta_{13} = |U_{e3}|^2, \quad \sin^2 \theta_{23} = \frac{|U_{\mu 3}|^2}{1 - |U_{e3}|^2}, \quad \sin^2 \theta_{12} = \frac{|U_{e2}|^2}{1 - |U_{e3}|^2}. \quad (\text{III.24})$$

Also, we compute the Jarlskog invariant, δ_{CP} derived from PMNS matrix elements $U_{\alpha i}$:

$$J_{CP} = \text{Im}[U_{e1}U_{\mu 2}U_{e2}^*U_{\mu 1}^*] = s_{23}c_{23}s_{12}c_{12}s_{13}c_{13}^2 \sin \delta_{CP}, \quad (\text{III.25})$$

where $s_{ij} \equiv \sin \theta_{ij}$ and $c_{ij} \equiv \cos \theta_{ij}$. The Majorana phases are found in terms of the following relations:

$$\text{Im}[U_{e1}^*U_{e2}] = c_{12}s_{12}c_{13}^2 \sin\left(\frac{\alpha_{21}}{2}\right), \quad \text{Re}[U_{e1}^*U_{e2}] = c_{12}s_{12}c_{13}^2 \cos\left(\frac{\alpha_{21}}{2}\right), \quad (\text{III.26})$$

$$\text{Im}[U_{e1}^*U_{e3}] = c_{12}s_{13}c_{13} \sin\left(\frac{\alpha_{31}}{2} - \delta_{CP}\right), \quad \text{Re}[U_{e1}^*U_{e3}] = c_{12}s_{13}c_{13} \cos\left(\frac{\alpha_{31}}{2} - \delta_{CP}\right), \quad (\text{III.27})$$

and $\alpha = \alpha_{21} - \alpha_{31}$. Using these mixings and phases, the neutrinoless double beta decay $\langle m_{ee} \rangle$ is described by

$$(\text{NH}) : \langle m_{ee} \rangle = \kappa |\tilde{D}_{\nu 2} s_{12}^2 c_{13}^2 e^{i\alpha} + \tilde{D}_{\nu 3} s_{13}^2 e^{-2i\delta_{CP}}|, \quad (\text{III.28})$$

$$(\text{IH}) : \langle m_{ee} \rangle = \kappa |\tilde{D}_{\nu 1} c_{12}^2 c_{13}^2 + \tilde{D}_{\nu 2} s_{12}^2 c_{13}^2 e^{i\alpha}|, \quad (\text{III.29})$$

and $\langle m_{ee} \rangle$ would be measured by future experiment of KamLAND-Zen [28].

D. Numerical analysis

We show our $\Delta\chi^2$ analysis, applying the neutrino oscillation data at 5σ intervals in NuFit6.0 [29] where Dirac CP phase is considered as an output parameter. Therefore, we have five fitting observables: $\Delta m_{\text{sol}}^2, \Delta m_{\text{atm}}^2, s_{12}, s_{13}, s_{23}$. The masses of charged-leptons are referred to ref. PDG[30]. Our input parameter is randomly selected within the following ranges:

$$|\tilde{b}_k| \in [0, 100], \quad \arg[\tilde{b}_k] \in [-\pi, +\pi], \quad (\text{III.30})$$

where modulus τ is within the range of the fundamental region. Since we do not have a solution within the range of 5σ in the case of IH, we shall now concentrate on discussing NH. Moreover, we have solutions with the range of $4 - 5\sigma$ and minimum $\Delta\chi^2$ is about 16.

	$\tau \simeq \omega$	$\tau = \omega$ ($\Delta\chi^2 \leq 10^3$)	Exp. ($\leq 3\sigma$) [29]
$\text{Re}[\tau]$	$[-0.496417, -0.495257]$	-0.5	—
$\text{Im}[\tau]$	$[0.869247, 0.872521]$	$\frac{\sqrt{3}}{2}$	—
$\text{Abs}[\tilde{b}_k]$	$[0.392093, 0.630404]$	$[72.3016, 94.8867]$	—
$ \text{Arg}[\tilde{b}_k] $	$[1.67832, 2.46345]$	$[1.48833, 2.69007]$	—
$\frac{\Delta m_{\text{sol}}^2}{[\text{eV}^2]} \times 10^5$	$[7.07173, 8.09637]$	$[4.40984, 9.83044]$	$[6.92, 8.05]$
s_{13}^2	$[0.0209175, 0.023878]$	$[0.0145046, 0.0309362]$	$[0.02023, 0.02376]$
s_{23}^2	$[0.430074, 0.440551]$	$[0.248265, 0.286931]$	$[0.430, 0.596]$
s_{12}^2	$[0.35123, 0.377646]$	$[0.541366, 0.549013]$	$[0.275, 0.345]$
$\Delta\chi_{\text{min}}^2$	16.0067	786.129	—

TABLE II: Allowed regions for our input and observed parameters for NH. Here, the value of atmospheric mass square difference runs over whole the experimental regions $\frac{\Delta m_{\text{atm}}^2}{[\text{eV}^2]} \times 10^3 = [2.463, 2.606]$ at 3σ range [29].

Thus, all the plots are within this range. In comparison, we also show some figures at $\tau = \omega$ where the upper bound on $\Delta\chi^2$ is restricted to a maximum of 1,000. Moreover, we have found that the minimum of $\Delta\chi^2$ is 786.129 at $\tau = \omega$; that is,

$$786.129 \leq \Delta\chi^2 \leq 1000. \quad (\text{III.31})$$

We summarize each case of $\Delta\chi^2$ in Tab. II.

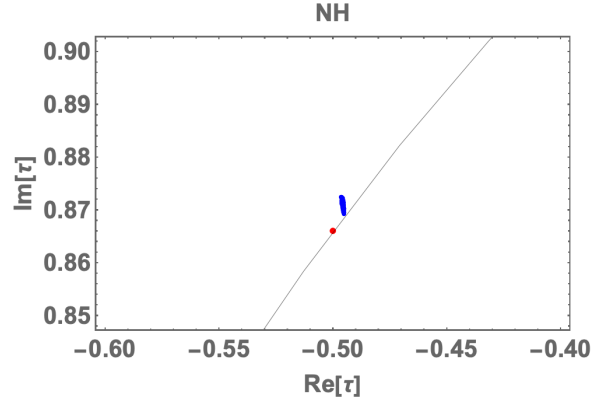


FIG. 1: Allowed region in terms of real τ and imaginary τ . The blue points are localized at the region at nearby $\omega \equiv e^{2\pi i}$ where red point is $\tau = \omega$

Fig. 1 shows the allowed region of τ within the fundamental region where the blue points

are localized at the region nearby $\omega \equiv e^{2\pi i}$. The red point represents $\tau = \omega$. Interestingly, τ is very close to ω . The absolute value of deviation from the $\tau = \omega$ is about 0.006. We also show the allowed ranges of our input parameters τ and \tilde{b}_k in Tab. II through our numerical analysis. In case of $\tau \simeq \omega$, $|\tilde{b}_k| \approx [0.39, 0.63]$ and $|\text{Arg}[b_k]| \approx [1.68, 2.46]$ are requested which is rather localized compared to our parameter space in Eq. (III.30). On the other hand, order 100 of $|\tilde{b}_k|$ is favored in case of $\tau = \omega$.

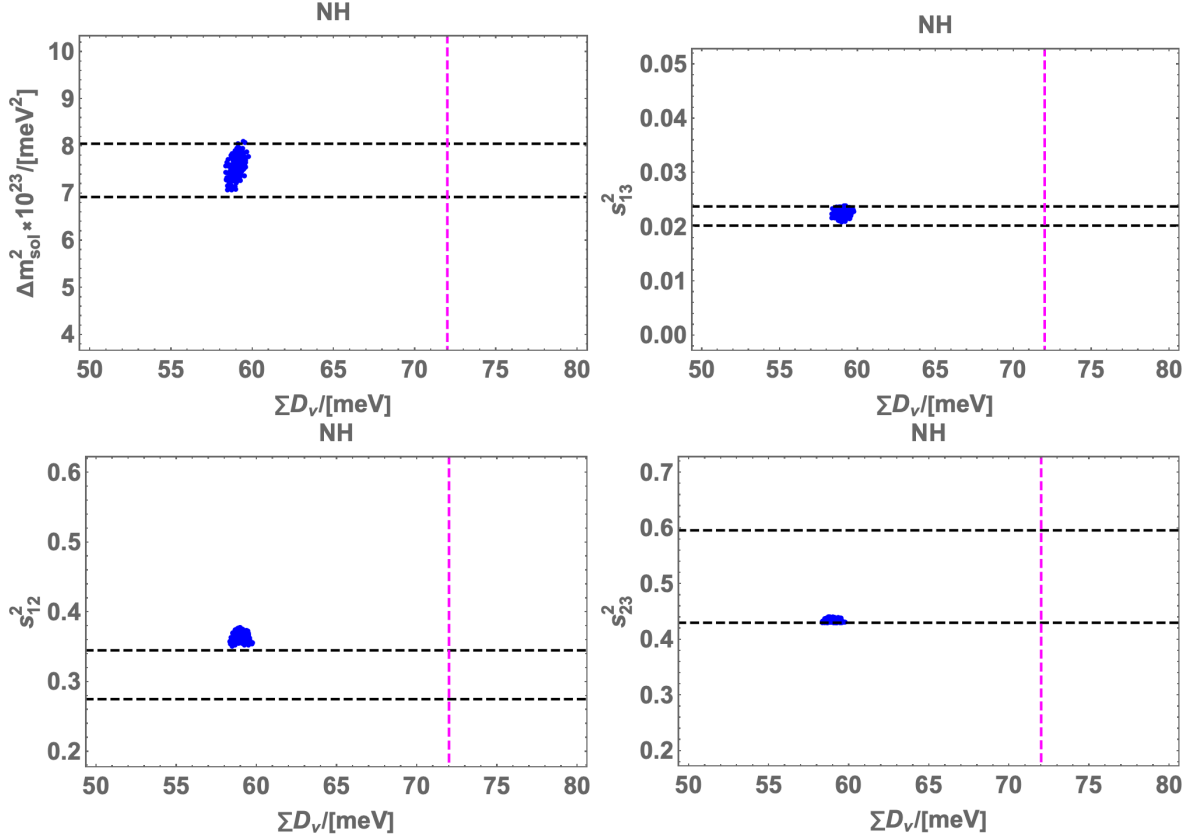


FIG. 2: Blue points are our allowed regions of Δm_{sol}^2 (up-left), s_{13}^2 (up-right), s_{12}^2 (down-left), and s_{23}^2 (down-right) in terms of $\sum D_\nu$. Each dotted horizontal black line represents experimental upper(lower)-bound at 3σ interval where these lines are given by two dimensional χ^2 analysis. The vertical magenta dotted line shows the upper bound on $\sum D_\nu \leq 72$ eV from the combined result of DESI and CMB.

Fig. 2 shows our allowed regions (with blue points) of Δm_{sol}^2 (up-left), s_{13}^2 (up-right), s_{12}^2 (down-left), and s_{23}^2 (down-right) in terms of $\sum D_\nu$. Each dotted horizontal black line represents experimental upper(lower)-bound at 3σ interval where these lines are given by two dimensional χ^2 analysis. The vertical magenta dotted line shows the upper bound on

$\sum D_\nu \leq 72$ eV from the combined result of DESI and CMB. The range of $\sum D_\nu$ is about [58-60] meV that is nothing but the direct result of Eq. (III.22). These figures suggest that Δm_{sol}^2 and s_{13}^2 almost run within the whole range of experimental ranges. But s_{23}^2 is localized near the lower experimental bound. s_{12}^2 is slightly deviated from the upper experimental bound. ⁵ In Tab. II, we show allowed ranges for these observables for $\tau \simeq \omega$, $\tau = \omega$, and experimental results at 3σ interval. Even in case of $\tau = \omega$, our model satisfies two experimental values of Δm_{sol}^2 and s_{13}^2 which are also well-fitted in case of $\tau \simeq \omega$. But s_{23}^2 and s_{12}^2 at $\tau = \omega$ are largely deviated from the lower and upper bound of experimental results, respectively. This implies that deviation from $\tau = \omega$, whose absolute value is ~ 0.006 , plays a crucial role in fitting these two mixings of s_{23}^2 and s_{12}^2 .

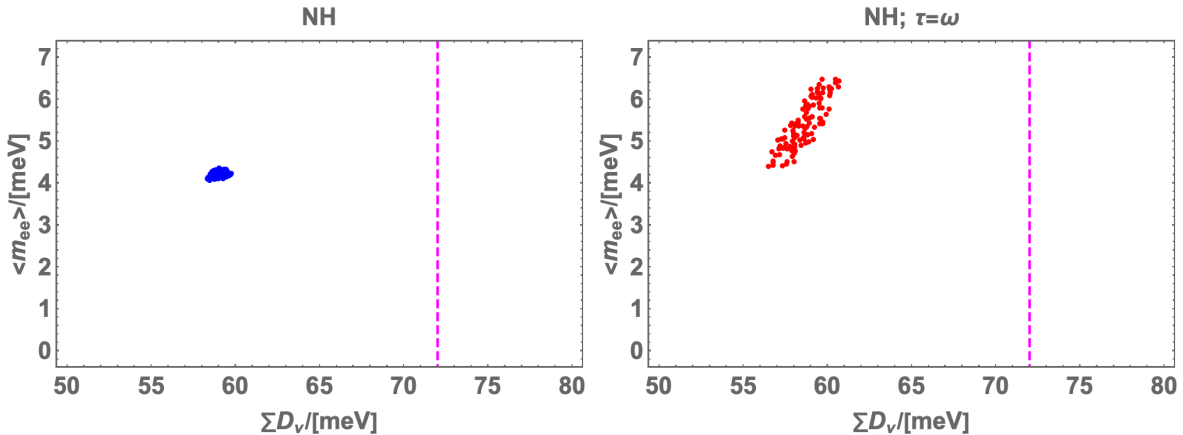


FIG. 3: Allowed region for the neutrinoless double beta decay in terms of sum of neutrino masses. The legend of colors are the same as Fig.1. The vertical dotted line is the upper bound on DESI and CMB data combination.

Fig. 3 shows allowed region between $\langle m_{ee} \rangle$ and $\sum D_\nu$ in meV unit, where the legends of colors are the same as Fig. 1. The vertical dotted line is the upper bound on DESI and CMB data combination. While the range of $\langle m_{ee} \rangle$ is about [4-4.4](4.3-6.5) meV for $\tau \simeq \omega$ ($\tau = \omega$) which is much below the current upper bound.

Fig. 4 shows correlation between δ_{CP} and α , where the legend of colors are the same as Fig.1. It reads that Majorana phase tends to be localized at the range of [0, 65] deg, while

⁵ Our analysis is computed via five dimensional χ^2 analysis and this deviation does not mean our model is ruled out by the experimental result(that is calculated by two dimensional analysis).

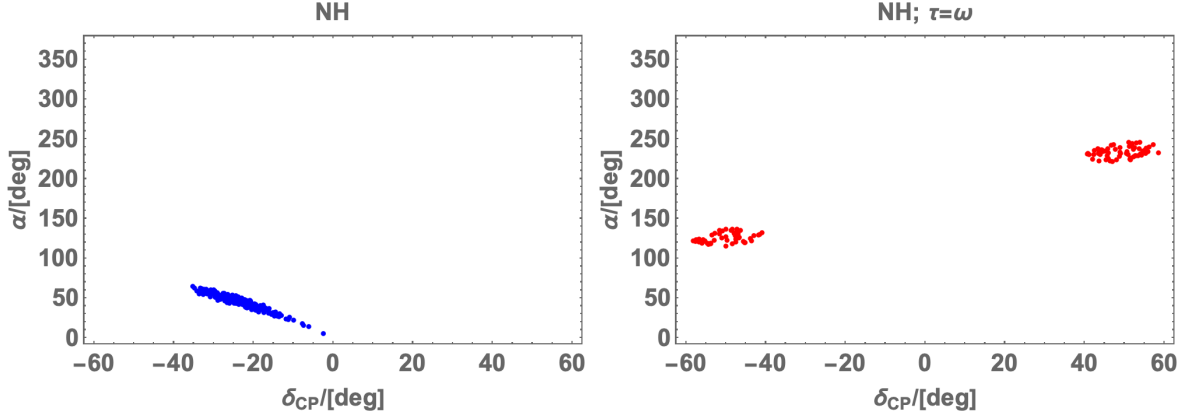


FIG. 4: The scatter plots for the Majorana phase α in terms of Dirac CP phase δ_{CP} . The legend of colors are the same as Fig.1.

the range of Dirac CP phase is about $[-35, 0]$ deg in case of $\tau \simeq \omega$.⁶ There are two localized islands in case of $\tau = \omega$; $[-60, -40]$, $[120, 140]$ and $[40, 60]$, $[230, 250]$ for Dirac CP phase and Majorana phase respectively.

IV. MODULUS STABILIZATION

As shown in the previous section, our model leads to realistic results at nearby $\tau = \omega$. In this section, we discuss the modulus stabilization to realize such a value. In these years, modulus stabilization has been studied within the framework of supersymmetric modular flavor models [31–40]. Some of those scenarios lead to the modulus stabilization at $\tau = \omega$. Here, we study modulus stabilization in a non-supersymmetric model leading to $\tau = \omega$.

For our purpose, it is important to understand the behavior of modular forms around $\tau = \omega$. The point $\tau = \omega$ is the fixed point of the ST transformation, and the \mathbb{Z}_3 symmetry remains. Under the ST transformation, the modular form transforms as

$$Y_{\mathbf{r}}^{(k)}(ST\tau) = (-\tau - 1)^k \rho_{\mathbf{r}}(ST) Y_{\mathbf{r}}^{(k)}(\tau). \quad (\text{IV.1})$$

It is convenient to use the parameter u [41],

$$u \equiv \frac{\tau - \omega}{\tau - \omega^2}. \quad (\text{IV.2})$$

⁶ If we include the case of $\tau \simeq -\omega^2$, our allowed region becomes to be symmetric.

We also use its complex conjugate \bar{u} ,

$$\bar{u} \equiv \frac{\bar{\tau} - \omega^2}{\bar{\tau} - \omega}, \quad (\text{IV.3})$$

when we discuss non-holomorphic modular forms. In addition, we define

$$\hat{Y}_{\mathbf{r}}^{(k)}(u) = (1 - u)^{-k} Y_{\mathbf{r}}^{(k)}(\tau). \quad (\text{IV.4})$$

Then, its transformation behavior under ST is written as

$$\hat{Y}_{\mathbf{r}}^{(k)}(\omega^2 u) = \omega^{-k} \rho_{\mathbf{r}}(ST) \hat{Y}_{\mathbf{r}}^{(k)}(u). \quad (\text{IV.5})$$

Let us focus on A_4 singlets, i.e., $\mathbf{r} = \mathbf{1}, \mathbf{1}', \mathbf{1}''$. Under ST , They transform as

$$\hat{Y}_{\mathbf{r}}^{(k)}(\omega^2 u) = \omega^{q_r - k} \hat{Y}_{\mathbf{r}}^{(k)}(u), \quad (\text{IV.6})$$

where $q_r = 0, 1, 2$ for $\mathbf{r} = \mathbf{1}, \mathbf{1}', \mathbf{1}''$, respectively. Furthermore, their ℓ -derivatives satisfy the following equations:

$$(\omega^{2\ell} - \omega^{q_r - k}) \left. \frac{d^\ell \hat{Y}_{\mathbf{r}}^{(k)}}{du^\ell} \right|_{u=\bar{u}=0} = 0, \quad (\text{IV.7})$$

$$(\omega^\ell - \omega^{q_r - k}) \left. \frac{d^\ell \hat{Y}_{\mathbf{r}}^{(k)}}{d\bar{u}^\ell} \right|_{u=\bar{u}=0} = 0. \quad (\text{IV.8})$$

That implies that

$$\left. \frac{d^\ell \hat{Y}_{\mathbf{r}}^{(k)}}{du^\ell} \right|_{u=0} = 0, \quad (\text{IV.9})$$

unless $2\ell = q_r - k = 0 \pmod{3}$, and

$$\left. \frac{d^\ell \hat{Y}_{\mathbf{r}}^{(k)}}{d\bar{u}^\ell} \right|_{u=\bar{u}=0} = 0, \quad (\text{IV.10})$$

unless $\ell = q_r - k = 0 \pmod{3}$. By use of these results, we can expand the modular forms around $\tau = \omega$. See Appendix B for its detail. For example, we can expand $Y_{\mathbf{1}}^{(4)}$ as

$$Y_{\mathbf{1}}^{(4)}(\tau) = -\frac{i}{\sqrt{3}} \left. \frac{d\hat{Y}_{\mathbf{1}}^{(4)}}{du} \right|_{u=0} (\tau - \omega) + \frac{8}{3} \left. \frac{d\hat{Y}_{\mathbf{1}}^{(4)}}{du} \right|_{u=0} (\tau - \omega)^2 + \mathcal{O}((\tau - \omega)^3). \quad (\text{IV.11})$$

Note that $Y_{\mathbf{1}}^{(4)}(\tau = \omega) = 0$.

Now, let discuss the modulus stabilization by use of the above expansion of the modular forms. Here, we use the unit $\Lambda = 1$, where Λ is a typical mass scale of the modulus stabilization. We assume the following potential:

$$V(\tau, \bar{\tau}) = (2\text{Im}\tau)^4 |Y_{\mathbf{1}}^{(4)}(\tau)|^2. \quad (\text{IV.12})$$

That is modular invariant. It also satisfies the stationary condition:

$$\frac{\partial V}{\partial \tau} = \frac{\partial V}{\partial \bar{\tau}} = 0, \quad (\text{IV.13})$$

at $\tau = \omega$. In addition, we can calculate its second derivatives at $\tau = \omega$ as

$$\frac{\partial^2 V}{\partial \tau \partial \bar{\tau}} = 3 \left| \frac{d\hat{Y}_{\mathbf{1}}^{(4)}}{du} \right|_{u=0}^2 > 0, \quad \frac{\partial^2 V}{\partial \tau \partial \tau} = \frac{\partial^2 V}{\partial \bar{\tau} \partial \bar{\tau}} = 0. \quad (\text{IV.14})$$

Thus, this potential has the minimum at $\tau = \omega$.

We have many varieties of modular invariant potential terms to choose. For example, instead of $Y_{\mathbf{1}}^{(4)}(\tau)$, we can use other moduli forms $Y_{\mathbf{r}}^{(k)}(\tau)$ in the potential (IV.12) with proper powers of $(2\text{Im}\tau)$. If $Y_{\mathbf{r}}^{(k)}(\tau = \omega) = 0$ and its first derivative does not vanish, the results are the same and the modulus is stabilized at $\tau = \omega$. However, if we choose the modular forms $Y_{\mathbf{r}}^{(k)}(\tau)$, which satisfies $Y_{\mathbf{r}}^{(k)}(\tau = \omega) \neq 0$ as well as non-vanishing first derivatives, and use the following potential:

$$v(\tau, \bar{\tau}) = (2\text{Im}\tau)^{2k} |Y_{\mathbf{r}}^{(k)}(\tau)|^2, \quad (\text{IV.15})$$

the modulus is not be stabilized at $\tau = \omega$. We need a proper choice of the potential term. Furthermore, the following combination of potential terms:

$$\begin{aligned} \tilde{V}(\tau, \bar{\tau}) &= V(\tau, \bar{\tau}) + \varepsilon v(\tau, \bar{\tau}) \\ &= (2\text{Im}\tau)^4 |Y_{\mathbf{1}}^{(4)}(\tau)|^2 + \varepsilon (2\text{Im}\tau)^{2k} |Y_{\mathbf{r}}^{(k)}(\tau)|^2, \end{aligned} \quad (\text{IV.16})$$

is also modular invariant. Suppose $|\varepsilon| \ll 1$. Then, the stationary condition $\partial \tilde{V} / \partial \tau = \partial \tilde{V} / \partial \bar{\tau} = 0$ is approximated around $\tau = \omega$ as

$$\frac{\partial^2 V}{\partial \tau \partial \bar{\tau}} \delta \bar{\tau} + \varepsilon \frac{\partial v}{\partial \tau} = 0, \quad \frac{\partial^2 V}{\partial \tau \partial \bar{\tau}} \delta \tau + \varepsilon \frac{\partial v}{\partial \bar{\tau}} = 0, \quad (\text{IV.17})$$

where $\delta \tau$ denotes a small deviation from $\tau = \omega$, i.e., $\tau = \omega + \delta \tau$. Thus, by tuning ε , a small deviation from $\tau = \omega$ would be possible.

Another possibility for realizing a small deviation would be radiative corrections. When we add proper effects, we may realize a small deviation. For example, radiative corrections studied in ref. [42] can lead to a small deviation.⁷ In the model, A_4 modular forms of the weight 8 with the representations $\mathbf{1}'$ and $\mathbf{1}''$ were used. In addition, the model in ref. [42] corresponds to softly supersymmetry breaking model. Thus, we replace the supersymmetric mass by the fermionic mass and the combination of supersymmetric mass squared and supersymmetric breaking mass squared by the bosonic mass squared. Then, we can realize a small deviation from $\tau = \omega$ by choosing proper values of parameters. In ref. [45], a different type of corrections due to non-perturbative effects was studied. Such corrections may lead to a small deviation from $\tau = \omega$.

V. CONCLUSIONS AND DISCUSSIONS

We have studied the Zee-Babu model with a non-holomorphic modular A_4 symmetry, and we have constructed the model so that there are minimum free parameters (two complex parameters). In this case, we have found only the normal hierarchy is allowed that is the same result of A_1 texture, although the structure of the charged-lepton mass matrix is different from each other. Moreover, the allowed region to satisfy the neutrino oscillation data is localized at nearby $\tau = \omega$. The small absolute deviation, which is about 0.006, plays a crucial role in fitting these two mixings of s_{23}^2 and s_{12}^2 . In addition, we have obtained several predictions on Majorana and Dirac CP phases, and neutrinoless double beta decay as shown in our numerical analysis. Also, we have studied the modulus stabilization within the framework of non-supersymmetric models. Our modulus potential leads to the modulus stabilization at $\tau = \omega$. A small deviation may be possible from $\tau = \omega$ by including proper corrections on the modulus potential. In the end, we have calculated the expansion of modular forms at nearby $\tau = \omega$ in the Appendix B so that one can apply them for a model and understand its analytical structure when one obtains the allowed region at nearby this fixed point.

⁷ See also refs. [43, 44] for radiative corrections.

Acknowledgments

This work was supported in part JSPS KAKENHI Grant Numbers JP23K03375 (T.K.).

Appendix A: Concrete A_4 modular forms

Here, we write down concrete A_4 modular forms in term of $q \equiv e^{2\pi i\tau}$ expansion [10].

$Y_3^{(0)} \equiv [y_1, y_2, y_3]^T$ is given by the following forms

$$y_1 = y - \frac{3e^{-4\pi y}}{\pi q} - \frac{9e^{-8\pi y}}{2\pi q^2} - \frac{e^{-12\pi y}}{\pi q^3} - \frac{21e^{-16\pi y}}{4\pi q^4} - \frac{18e^{-20\pi y}}{5\pi q^5} - \frac{3e^{-24\pi y}}{2\pi q^6} + \dots$$

$$- \frac{9 \ln 3}{4\pi} - \frac{3q}{\pi} - \frac{9q^2}{2\pi} - \frac{q^3}{\pi} - \frac{21q^4}{4\pi} - \frac{18q^5}{5\pi} - \frac{3q^6}{2\pi} + \dots, \quad (\text{A.1})$$

$$y_2 = \frac{27q^{1/3}e^{\pi y/3}}{\pi} \left(\frac{e^{-3\pi y}}{4q} + \frac{e^{-7\pi y}}{5q^2} + \frac{5e^{-11\pi y}}{16q^3} + \frac{2e^{-15\pi y}}{11q^4} + \frac{2e^{-19\pi y}}{7q^5} + \frac{4e^{-23\pi y}}{17q^6} + \dots \right)$$

$$+ \frac{9q^{1/3}}{2\pi} \left(1 + \frac{7q}{4} + \frac{8q^2}{7} + \frac{9q^3}{5} + \frac{14q^4}{13} + \frac{31q^5}{16} + \frac{20q^6}{19} + \dots \right), \quad (\text{A.2})$$

$$y_3 = \frac{9q^{2/3}e^{2\pi y/3}}{2\pi} \left(\frac{e^{-2\pi y}}{q} + \frac{7e^{-6\pi y}}{4q^2} + \frac{8e^{-10\pi y}}{7q^3} + \frac{9e^{-14\pi y}}{5q^4} + \frac{14e^{-18\pi y}}{13q^5} + \frac{31e^{-22\pi y}}{16q^6} + \dots \right)$$

$$+ \frac{27q^{2/3}}{\pi} \left(\frac{1}{4} + \frac{q}{5} + \frac{5q^2}{16} + \frac{2q^3}{11} + \frac{2q^4}{7} + \frac{9q^5}{17} + \frac{21q^6}{20} + \dots \right), \quad (\text{A.3})$$

where $y \equiv \text{Im}[\tau]$ and $Y_1^{(0)} = 1$. $Y_3^{(-2)} \equiv [y'_1, y'_2, y'_3]^T$ is given by the following forms

$$y'_1 = \frac{y^3}{3} + \frac{21\Gamma_3(4\pi y)}{16\pi^3 q} + \frac{189\Gamma_3(8\pi y)}{128\pi^3 q^2} + \frac{169\Gamma_3(12\pi y)}{144\pi^3 q^3} + \frac{1533\Gamma_3(16\pi y)}{1024\pi^3 q^4} + \dots$$

$$+ \frac{\pi}{40} \frac{\zeta(3)}{\zeta(4)} + \frac{21q}{8\pi^3} + \frac{189q^2}{64\pi^3} + \frac{169q^3}{72\pi^3} + \frac{1533q^4}{512\pi^3} + \frac{1323q^5}{500\pi^3} + \frac{169q^6}{64\pi^3} + \dots, \quad (\text{A.4})$$

$$y'_2 = -\frac{729q^{1/3}}{16\pi^3} \left(\frac{\Gamma_3(8\pi y/3)}{16q} + \frac{7\Gamma_3(20\pi y/3)}{125q^2} + \frac{65\Gamma_3(32\pi y/3)}{1024q^3} + \frac{74\Gamma_3(44\pi y/3)}{1331q^4} + \dots \right)$$

$$- \frac{81q^{1/3}}{16\pi^3} \left(1 + \frac{73q}{64} + \frac{344q^2}{343} + \frac{567q^3}{500} + \frac{20198q^4}{2197} + \frac{4681q^5}{4096} + \dots \right), \quad (\text{A.5})$$

$$y'_3 = -\frac{81q^{2/3}}{32\pi^3} \left(\frac{\Gamma_3(4\pi y/3)}{q} + \frac{73\Gamma_3(16\pi y/3)}{64q^2} + \frac{344\Gamma_3(28\pi y/3)}{343q^3} + \frac{567\Gamma_3(40\pi y/3)}{500q^4} + \dots \right)$$

$$- \frac{729q^{2/3}}{8\pi^3} \left(\frac{1}{16} + \frac{7q}{125} + \frac{65q^2}{1024} + \frac{74q^3}{1331} + \dots \right), \quad (\text{A.6})$$

where $\Gamma_3(z) \approx (z^2 + 2z + 2)e^{-z}$. The singlet with modular weight -2 ; $Y_1^{(-2)}$, is given by

$$Y_1^{(-2)} = \frac{y^3}{3} - \frac{15\Gamma_3(4\pi y)}{4\pi^3 q} - \frac{135\Gamma_3(8\pi y)}{32\pi^3 q^2} - \frac{35\Gamma_3(12\pi y)}{9\pi^3 q^3} + \dots$$

$$- \frac{\pi}{12} \frac{\zeta(3)}{\zeta(4)} - \frac{15q}{2\pi^3} - \frac{135q^2}{16\pi^3} - \frac{70q^3}{9\pi^3} - \frac{1095q^4}{128\pi^3} - \frac{189q^5}{25\pi^3} - \frac{35q^6}{4\pi^3} + \dots. \quad (\text{A.7})$$

$Y_3^{(2)} \equiv [f_1, f_2, f_3]^T$ is given by the following forms [4]:

$$f_1 = 1 + 12q + 36q^2 + 12q^3 + 84q^4 + 72q^5 + \dots, \quad (\text{A.8})$$

$$f_2 = -6q^{1/3} (1 + 7q + 8q^2 + 18q^3 + 14q^4 + \dots), \quad (\text{A.9})$$

$$f_3 = -18q^{2/3} (1 + 2q + 5q^2 + 4q^3 + 8q^4 + \dots). \quad (\text{A.10})$$

Then, the modular forms with 4 modular weights can be obtained via A_4 multiplication rules [20] and their forms are as follows:

$$Y_3^{(4)} = [f_1^2 - f_2 f_3, f_3^2 - f_1 f_2, f_2^2 - f_1 f_3]^T, \quad (\text{A.11})$$

$$Y_1^{(4)} = f_1^2 + 2f_2 f_3, \quad Y_{1'}^{(4)} = f_3^2 + 2f_1 f_2, \quad (\text{A.12})$$

where $Y_{1''}^{(4)} = 0$. Finally, the singlet modular forms with 8 weight is constructed by the ones of 4 modular weights as follows:

$$Y_1^{(8)} = (f_1^2 + 2f_2 f_3)^2, \quad Y_{1'}^{(8)} = (f_1^2 + 2f_2 f_3)(f_3^2 + 2f_1 f_2), \quad Y_{1''}^{(8)} = (f_3^2 + 2f_1 f_2)^2. \quad (\text{A.13})$$

Appendix B: A_4 modular forms and their derivatives

In our paper, it is too difficult to *analytically* understand how the deviation from $\tau = \omega$ contributes to neutrino observables. However, it would be worthwhile for us to discuss expansion modular Yukawa forms in terms of the deviation. We expect *in the future* that this forms would be helpful to understand analytical predictions for quark and lepton masses and mixings when one obtains solutions at nearby fixed points in framework of non-holomorphic modular symmetries.⁸

The modular symmetry transforms the modular form as

$$Y_{\mathbf{r}}^{(k)}(\gamma\tau, \overline{\gamma\tau}) = (c\tau + d)^k \rho_{\mathbf{r}}(\gamma) Y_{\mathbf{r}}^{(k)}(\tau, \bar{\tau}). \quad (\text{B.1})$$

In order to show the behavior of modular form around $\tau = \omega$, it is convenient to use the parameters u and \bar{u} ,

$$u \equiv \frac{\tau - \omega}{\tau - \omega^2}, \quad \bar{u} \equiv \frac{\bar{\tau} - \omega^2}{\bar{\tau} - \omega}. \quad (\text{B.2})$$

⁸ In whole the calculations in case of holomorphic case, refs. [39, 41, 42] are helpful.

The parameters u and \bar{u} transform to $\omega^2 u$ and $\omega \bar{u}$ by ST . Also we define

$$\hat{Y}_{\mathbf{r}}^{(k)}(u, \bar{u}) = (1 - u)^{-k} Y_{\mathbf{r}}^{(k)}(\tau, \bar{\tau}). \quad (\text{B.3})$$

Then, its transformation behavior under ST is written as

$$\hat{Y}_{\mathbf{r}}^{(k)}(\omega^2 u, \omega \bar{u}) = \omega^{-k} \rho_{\mathbf{r}}(ST) \hat{Y}_{\mathbf{r}}^{(k)}(u, \bar{u}). \quad (\text{B.4})$$

When we focus on $\mathbf{r} = \mathbf{1}, \mathbf{1}', \mathbf{1}''$, this transformation behavior can be written by

$$\hat{Y}_{\mathbf{r}}^{(k)}(\omega^2 u, \omega \bar{u}) = \omega^{q_r - k} \hat{Y}_{\mathbf{r}}^{(k)}(u, \bar{u}), \quad (\text{B.5})$$

where $q_r = 0, 1, 2$ for $\mathbf{r} = \mathbf{1}, \mathbf{1}', \mathbf{1}''$, respectively. We take the ℓ -derivative of the above equation so as to obtain

$$(\omega^{2\ell} - \omega^{q_r - k}) \left. \frac{d^\ell \hat{Y}_{\mathbf{r}}^{(k)}}{du^\ell} \right|_{u=\bar{u}=0} = 0, \quad (\text{B.6})$$

$$(\omega^\ell - \omega^{q_r - k}) \left. \frac{d^\ell \hat{Y}_{\mathbf{r}}^{(k)}}{d\bar{u}^\ell} \right|_{u=\bar{u}=0} = 0. \quad (\text{B.7})$$

Next, we discuss $\mathbf{r} = \mathbf{3}$. The transformation behavior can be written by

$$\hat{Y}_{\mathbf{3}}^{(k)}(\omega^2 u, \omega \bar{u}) = \omega^{-k} \rho_{\mathbf{3}}(ST) \hat{Y}_{\mathbf{3}}^{(k)}(u, \bar{u}), \quad (\text{B.8})$$

where

$$\rho_{\mathbf{3}}(ST) = \frac{1}{3} \begin{pmatrix} -1 & 2\omega & 2\omega^2 \\ 2 & -\omega & 2\omega^2 \\ 2 & 2\omega & -\omega^2 \end{pmatrix}. \quad (\text{B.9})$$

The eigenvalues and the eigenvectors are

$$1 : v_1 = \frac{1}{3}(-\omega, 2\omega^2, 2)^T, \quad (\text{B.10})$$

$$\omega : v_\omega = \frac{1}{3}(2\omega, -\omega^2, 2)^T, \quad (\text{B.11})$$

$$\omega^2 : v_{\omega^2} = \frac{1}{3}(-2\omega, -2\omega^2, 1)^T. \quad (\text{B.12})$$

$$\hat{Y}_{\mathbf{3}}^{(k)} = \sum_{i=(1,\omega,\omega^2)} a_i^{(k)} v_i, \quad (\text{B.13})$$

where $v_i^\dagger v_j = \delta_{ij}$ and $a_i^{(k)} = v_i^\dagger \hat{Y}_3^{(k)}$. We take the ℓ -derivative of the above equation

$$\omega^{2\ell} \left. \frac{d^\ell \hat{Y}_3^{(k)}}{du^\ell} \right|_{u=\bar{u}=0} = \omega^{-k} \rho_3(ST) \left. \frac{d^\ell \hat{Y}_3^{(k)}}{du^\ell} \right|_{u=\bar{u}=0} \quad (\text{B.14})$$

$$= \omega^{-k} \rho_3(ST) \sum_{i=(1,\omega,\omega^2)} \left. \frac{d^\ell a_i^{(k)}}{du^\ell} \right|_{u=\bar{u}=0} v_i. \quad (\text{B.15})$$

and

$$\omega^\ell \left. \frac{d^\ell \hat{Y}_3^{(k)}}{d\bar{u}^\ell} \right|_{u=\bar{u}=0} = \omega^{-k} \rho_3(ST) \left. \frac{d^\ell \hat{Y}_3^{(k)}}{d\bar{u}^\ell} \right|_{u=\bar{u}=0} \quad (\text{B.16})$$

$$= \omega^{-k} \rho_3(ST) \sum_{i=(1,\omega,\omega^2)} \left. \frac{d^\ell a_i^{(k)}}{d\bar{u}^\ell} \right|_{u=\bar{u}=0} v_i. \quad (\text{B.17})$$

We can obtain the following equations,

$$(\omega^{2\ell} - \omega^{q_i-k}) \left. \frac{d^\ell a_i^{(k)}}{du^\ell} \right|_{u=\bar{u}=0} = 0, \quad (\omega^\ell - \omega^{q_i-k}) \left. \frac{d^\ell a_i^{(k)}}{d\bar{u}^\ell} \right|_{u=\bar{u}=0} = 0. \quad (\text{B.18})$$

$k \equiv 0 \pmod{3}$ case

$$\frac{d^\ell \hat{Y}_3^{(k)}}{du^\ell} = \begin{cases} \frac{d^\ell a_1^{(k)}}{du^\ell} v_1 & (\ell \equiv 0 \pmod{3}) \\ \frac{d^\ell a_{\omega^2}^{(k)}}{du^\ell} v_{\omega^2} & (\ell \equiv 1 \pmod{3}) \\ \frac{d^\ell a_\omega^{(k)}}{du^\ell} v_\omega & (\ell \equiv 2 \pmod{3}) \end{cases} \quad (\text{B.19})$$

$$\frac{d^\ell \hat{Y}_3^{(k)}}{d\bar{u}^\ell} = \begin{cases} \frac{d^\ell a_1^{(k)}}{d\bar{u}^\ell} v_1 & (\ell \equiv 0 \pmod{3}) \\ \frac{d^\ell a_\omega^{(k)}}{d\bar{u}^\ell} v_\omega & (\ell \equiv 1 \pmod{3}) \\ \frac{d^\ell a_{\omega^2}^{(k)}}{d\bar{u}^\ell} v_{\omega^2} & (\ell \equiv 2 \pmod{3}) \end{cases} \quad (\text{B.20})$$

$k \equiv 1 \pmod{3}$ case

$$\frac{d^\ell \hat{Y}_3^{(k)}}{du^\ell} = \begin{cases} \frac{d^\ell a_\omega^{(k)}}{du^\ell} v_\omega & (\ell \equiv 0 \pmod{3}) \\ \frac{d^\ell a_1^{(k)}}{du^\ell} v_1 & (\ell \equiv 1 \pmod{3}) \\ \frac{d^\ell a_{\omega^2}^{(k)}}{du^\ell} v_{\omega^2} & (\ell \equiv 2 \pmod{3}) \end{cases} \quad (\text{B.21})$$

$$\frac{d^\ell \hat{Y}_3^{(k)}}{d\bar{u}^\ell} = \begin{cases} \frac{d^\ell a_\omega^{(k)}}{d\bar{u}^\ell} v_\omega & (\ell \equiv 0 \pmod{3}) \\ \frac{d^\ell a_{\omega^2}^{(k)}}{d\bar{u}^\ell} v_{\omega^2} & (\ell \equiv 1 \pmod{3}) \\ \frac{d^\ell a_1^{(k)}}{d\bar{u}^\ell} v_1 & (\ell \equiv 2 \pmod{3}) \end{cases} \quad (\text{B.22})$$

$k \equiv 2 \pmod{3}$ case

$$\frac{d^\ell \hat{Y}_3^{(k)}}{du^\ell} = \begin{cases} \frac{d^\ell a_{\omega^2}^{(k)}}{du^\ell} v_{\omega^2} & (\ell \equiv 0 \pmod{3}) \\ \frac{d^\ell a_\omega^{(k)}}{du^\ell} v_\omega & (\ell \equiv 1 \pmod{3}) \\ \frac{d^\ell a_1^{(k)}}{du^\ell} v_1 & (\ell \equiv 2 \pmod{3}) \end{cases} \quad (\text{B.23})$$

$$\frac{d^\ell \hat{Y}_3^{(k)}}{d\bar{u}^\ell} = \begin{cases} \frac{d^\ell a_{\omega^2}^{(k)}}{d\bar{u}^\ell} v_{\omega^2} & (\ell \equiv 0 \pmod{3}) \\ \frac{d^\ell a_1^{(k)}}{d\bar{u}^\ell} v_1 & (\ell \equiv 1 \pmod{3}) \\ \frac{d^\ell a_\omega^{(k)}}{d\bar{u}^\ell} v_\omega & (\ell \equiv 2 \pmod{3}) \end{cases} \quad (\text{B.24})$$

$$\frac{du}{d\tau} = \frac{(u-1)^2}{i\sqrt{3}}, \quad \frac{d\bar{u}}{d\bar{\tau}} = -\frac{(\bar{u}-1)^2}{i\sqrt{3}}. \quad (\text{B.25})$$

The first and second derivatives of the modular form $Y_{\mathbf{r}}^{(k)}$ are written by

$$\frac{dY_{\mathbf{r}}^{(k)}}{d\tau} = \frac{(1-u)^{k+2}}{\sqrt{3}i} \left(\frac{d\hat{Y}_{\mathbf{r}}^{(k)}}{du} - \frac{k}{1-u} \hat{Y}_{\mathbf{r}}^{(k)} \right), \quad (\text{B.26})$$

$$\frac{d^2 Y_{\mathbf{r}}^{(k)}}{d\tau^2} = -\frac{(1-u)^{k+4}}{3} \left(\frac{d^2 \hat{Y}_{\mathbf{r}}^{(k)}}{du^2} - \frac{2(k+1)}{1-u} \frac{d\hat{Y}_{\mathbf{r}}^{(k)}}{du} + \frac{k(k+1)}{(1-u)^2} \hat{Y}_{\mathbf{r}}^{(k)} \right), \quad (\text{B.27})$$

$$\frac{dY_{\mathbf{r}}^{(k)}}{d\bar{\tau}} = -\frac{(1-u)^k (1-\bar{u})^2}{\sqrt{3}i} \frac{d\hat{Y}_{\mathbf{r}}^{(k)}}{d\bar{u}}, \quad (\text{B.28})$$

$$\frac{d^2 Y_{\mathbf{r}}^{(k)}}{d\bar{\tau}^2} = -\frac{(1-u)^k (1-\bar{u})^4}{3} \left(\frac{d^2 \hat{Y}_{\mathbf{r}}^{(k)}}{d\bar{u}^2} - \frac{2}{1-\bar{u}} \frac{d\hat{Y}_{\mathbf{r}}^{(k)}}{d\bar{u}} \right), \quad (\text{B.29})$$

$$\frac{d^2 Y_{\mathbf{r}}^{(k)}}{d\tau d\bar{\tau}} = \frac{(1-u)^{k+2} (1-\bar{u})^2}{3} \left(\frac{d^2 \hat{Y}_{\mathbf{r}}^{(k)}}{dud\bar{u}} - \frac{k}{1-u} \frac{d\hat{Y}_{\mathbf{r}}^{(k)}}{d\bar{u}} \right). \quad (\text{B.30})$$

By use of the above results, we can expand the modular form around $\tau = \omega$ and $\bar{\tau} = \omega^2$.

We can expand $Y_{\mathbf{r}}^{(k)}$ as

$$\begin{aligned} Y_{\mathbf{r}}^{(k)}(\tau, \bar{\tau}) &= \hat{Y}_{\mathbf{r}}^{(k)}(0, 0) - \frac{i}{\sqrt{3}} \left(\frac{d\hat{Y}_{\mathbf{r}}^{(k)}(0, 0)}{du} - k\hat{Y}_{\mathbf{r}}^{(k)}(0, 0) \right) (\tau - \omega) \\ &\quad + \frac{i}{\sqrt{3}} \frac{d\hat{Y}_{\mathbf{r}}^{(k)}(0, 0)}{d\bar{u}} (\bar{\tau} - \omega^2) + \mathcal{O}(|\tau - \omega|^2). \end{aligned} \quad (\text{B.31})$$

[1] A. Zee, Nucl. Phys. B **264**, 99 (1986).

- [2] K. S. Babu, Phys. Lett. B **203**, 132 (1988).
- [3] H. Fritzsch, Z.-z. Xing, and S. Zhou, JHEP **09**, 083 (2011), 1108.4534.
- [4] F. Feruglio, *Are neutrino masses modular forms?* (2019), pp. 227–266, 1706.08749.
- [5] T. Kobayashi, K. Tanaka, and T. H. Tatsuishi, Phys. Rev. D **98**, 016004 (2018), 1803.10391.
- [6] J. T. Penedo and S. T. Petcov, Nucl. Phys. B **939**, 292 (2019), 1806.11040.
- [7] P. P. Novichkov, J. T. Penedo, S. T. Petcov, and A. V. Titov, JHEP **04**, 174 (2019), 1812.02158.
- [8] T. Kobayashi and M. Tanimoto (2023), 2307.03384.
- [9] G.-J. Ding and S. F. King (2023), 2311.09282.
- [10] B.-Y. Qu and G.-J. Ding, JHEP **08**, 136 (2024), 2406.02527.
- [11] S. Kikuchi, T. Kobayashi, K. Nasu, H. Otsuka, S. Takada, and H. Uchida, PTEP **2022**, 123B02 (2022), 2203.14667.
- [12] T. Nomura and H. Okada (2024), 2408.01143.
- [13] G.-J. Ding, J.-N. Lu, S. T. Petcov, and B.-Y. Qu (2024), 2408.15988.
- [14] C.-C. Li, J.-N. Lu, and G.-J. Ding, JHEP **12**, 189 (2024), 2410.24103.
- [15] T. Nomura and H. Okada (2024), 2412.18095.
- [16] T. Nomura, H. Okada, and O. Popov, Phys. Lett. B **860**, 139171 (2025), 2409.12547.
- [17] H. Okada and Y. Orikasa (2025), 2501.15748.
- [18] R. de Adelhart Toorop, F. Feruglio, and C. Hagedorn, Nucl. Phys. B **858**, 437 (2012), 1112.1340.
- [19] G. Altarelli and F. Feruglio, Rev. Mod. Phys. **82**, 2701 (2010), 1002.0211.
- [20] H. Ishimori, T. Kobayashi, H. Ohki, Y. Shimizu, H. Okada, and M. Tanimoto, Prog. Theor. Phys. Suppl. **183**, 1 (2010), 1003.3552.
- [21] D. Hernandez and A. Y. Smirnov, Phys. Rev. D **86**, 053014 (2012), 1204.0445.
- [22] S. F. King and C. Luhn, Rept. Prog. Phys. **76**, 056201 (2013), 1301.1340.
- [23] S. F. King, A. Merle, S. Morisi, Y. Shimizu, and M. Tanimoto, New J. Phys. **16**, 045018 (2014), 1402.4271.
- [24] S. T. Petcov, Eur. Phys. J. C **78**, 709 (2018), 1711.10806.
- [25] T. Kobayashi, H. Ohki, H. Okada, Y. Shimizu, and M. Tanimoto, *An Introduction to Non-Abelian Discrete Symmetries for Particle Physicists* (2022), ISBN 978-3-662-64678-6, 978-3-662-64679-3.

- [26] A. G. Adame et al. (DESI) (2024), 2404.03002.
- [27] Z. Maki, M. Nakagawa, and S. Sakata, Prog. Theor. Phys. **28**, 870 (1962).
- [28] S. Abe et al. (KamLAND-Zen) (2024), 2406.11438.
- [29] I. Esteban, M. C. Gonzalez-Garcia, M. Maltoni, I. Martinez-Soler, J. a. P. Pinheiro, and T. Schwetz, JHEP **12**, 216 (2024), 2410.05380.
- [30] R. L. Workman et al. (Particle Data Group), PTEP **2022**, 083C01 (2022).
- [31] T. Kobayashi, Y. Shimizu, K. Takagi, M. Tanimoto, and T. H. Tatsuishi, Phys. Rev. D **100**, 115045 (2019), [Erratum: Phys.Rev.D 101, 039904 (2020)], 1909.05139.
- [32] T. Kobayashi, Y. Shimizu, K. Takagi, M. Tanimoto, T. H. Tatsuishi, and H. Uchida, Phys. Rev. D **101**, 055046 (2020), 1910.11553.
- [33] H. Abe, T. Kobayashi, S. Uemura, and J. Yamamoto, Phys. Rev. D **102**, 045005 (2020), 2003.03512.
- [34] K. Ishiguro, T. Kobayashi, and H. Otsuka, JHEP **03**, 161 (2021), 2011.09154.
- [35] P. P. Novichkov, J. T. Penedo, and S. T. Petcov, JHEP **03**, 149 (2022), 2201.02020.
- [36] V. Knapp-Perez, X.-G. Liu, H. P. Nilles, S. Ramos-Sanchez, and M. Ratz, Phys. Lett. B **844**, 138106 (2023), 2304.14437.
- [37] S. F. King and X. Wang, Phys. Rev. D **110**, 076026 (2024), 2310.10369.
- [38] S. Funakoshi, J. Kawamura, T. Kobayashi, K. Nasu, and H. Otsuka (2024), 2409.19261.
- [39] Y. Abe, K. Goto, T. Higaki, T. Kobayashi, and K. Nasu (2024), 2405.08316.
- [40] T. Higaki, T. Kobayashi, K. Nasu, and H. Otsuka, JHEP **09**, 024 (2024), 2405.18813.
- [41] P. P. Novichkov, J. T. Penedo, and S. T. Petcov, JHEP **04**, 206 (2021), 2102.07488.
- [42] T. Kobayashi, K. Nasu, R. Sakuma, and Y. Yamada, Phys. Rev. D **108**, 115038 (2023), 2310.15604.
- [43] T. Higaki, J. Kawamura, and T. Kobayashi, JHEP **04**, 147 (2024), 2402.02071.
- [44] T. Higaki, J. Kawamura, T. Kobayashi, K. Nasu, and R. Sakuma (2024), 2412.18435.
- [45] K. Ishiguro, H. Okada, and H. Otsuka, JHEP **09**, 072 (2022), 2206.04313.